

L. Aho-Mantila, X. Bonnin, D.P. Coster, C. Lowry, M. Wischmeier,
S. Brezinsek, G. Federici, the ASDEX Upgrade Team
and JET EFDA contributors

Model-Based Radiation Scalings for the ITER-Like Divertors of JET and ASDEX Upgrade

“This document is intended for publication in the open literature. It is made available on the understanding that it may not be further circulated and extracts or references may not be published prior to publication of the original when applicable, or without the consent of the Publications Officer, EFDA, Culham Science Centre, Abingdon, Oxon, OX14 3DB, UK.”

“Enquiries about Copyright and reproduction should be addressed to the Publications Officer, EFDA, Culham Science Centre, Abingdon, Oxon, OX14 3DB, UK.”

The contents of this preprint and all other JET EFDA Preprints and Conference Papers are available to view online free at www.iop.org/Jet. This site has full search facilities and e-mail alert options. The diagrams contained within the PDFs on this site are hyperlinked from the year 1996 onwards.

Model-Based Radiation Scalings for the ITER-Like Divertors of JET and ASDEX Upgrade

L. Aho-Mantila¹, X. Bonnin², D.P. Coster³, C. Lowry⁴, M. Wischmeier³,
S. Brezinsek⁵, G. Federici⁶, the ASDEX Upgrade Team
and JET EFDA contributors*

JET-EFDA, Culham Science Centre, OX14 3DB, Abingdon, UK

¹*VTT Technical Research Centre of Finland, FI-02044 VTT, Finland*

²*LSPM - CNRS, Université Paris 13, Sorbonne Paris Cité, F-93430 Villetaneuse, France*

³*Max-Planck Institut für Plasmaphysik, D-85748 Garching, Germany*

⁴*EFDA JET CSU, Culham Science Centre, OX14 3DB, Abingdon, UK*

⁵*Forschungszentrum Jülich, Institut für Energie- und Klimaforschung Plasmaphysik,
52425 Jülich, Germany*

⁶*EFDA PPP&T Department, D-85748 Garching, Germany*

** See annex of F. Romanelli et al, "Overview of JET Results",
(24th IAEA Fusion Energy Conference, San Diego, USA (2012)).*

Preprint of Paper to be submitted for publication in Proceedings of the
21st International Conference on Plasma Surface Interactions, Kanazawa, Japan
26th May 2014 – 30th May 2014

ABSTRACT

Effects of N-seeding in L-mode experiments in ASDEX Upgrade and JET are analysed numerically with the SOLPS5.0 code package. The modelling yields 3 qualitatively different radiative regimes with increasing N concentration, when initially attached divertor conditions are studied. The radiation pattern is observed to evolve asymmetrically, with radiation increasing first in the inner divertor, then in the outer divertor, and finally on closed field lines above the X-point. The scaling of the radiative regimes is observed to be sensitive to cross-field drifts and divertor geometry, and the scaling of the divertor radiated power with the divertor neutral density is similar to an experimental scaling law for H-mode radiation. The same parametric dependencies are not observed in simulations without drifts.

1. INTRODUCTION

Understanding how radiative edge plasma solutions scale from one tokamak to another is important for predicting power exhaust in a future fusion reactor. The influence of machine size and divertor geometry on N-seeded divertor plasmas has been studied recently in dedicated, ELMfree L-mode discharges in ASDEX Upgrade and JET [1]. In the present paper, we analyse the radiative divertor plasmas corresponding to these experiments using 2D SOLPS5.0 simulations. We compare the modelled parametric dependencies to an existing scaling law [2] and discuss the physics ingredients which influence the scaling of these radiative plasmas. The paper is organized as follows: Section 2 describes the modelling approach, Section 3 presents the simulation results and the scaling studies, and a brief summary is presented in Section 4.

2. APPROACH USED IN THE SCALING STUDIES

Scaling studies must consider at least two machines of different size. Our analysis is based on similar N-seeded L-mode plasmas performed in the ASDEX Upgrade and JET tokamaks [1], both of which have metallic plasma-facing components and an ITER-like, W-coated lower divertor. The larger device, JET, has additionally Be in the main chamber, compared to the full-W wall in ASDEX Upgrade. For diagnostic purposes, lower-single-null plasma configurations were used in both devices, with the outer strike point positioned on the horizontal target in JET, and on the vertical target in ASDEX Upgrade (shown in Figures 2-4).

On both devices, our studies focus on moderate D fuelling levels, which yield a lowrecycling regime in the outer divertor leg. In the absence of ELMs, W core contributions are low and the edge heating power is reduced by W radiation by less than 10%, which is within the uncertainty range of the measurements. The intrinsic impurities are limited to possibly small levels of C and O in ASDEX Upgrade, and Be in JET. In the present studies, we have neglected all intrinsic impurities, including W, assuming that their effects are small compared to those induced by N-seeding.

The present paper focuses on modelling the effects of N-seeding in the two experiments. The simulations have been performed with the SOLPS5.0 code package [3], which couples the plasma fluid code B2.5 with the Monte Carlo neutrals code Eirene (1999 version). This modelbased scaling

is done using the same physics assumptions for both devices, adjusting the model parameters as little as possible to fit the observations in a specific machine. An exception is made for the radial transport coefficients, which are not yet described by first-principle physics models, but have been fitted with ballooning (B^{-1} dependence) to match the low-field-side profile measurements in unseeded discharges. The predicted, steady-state effects of N-seeding are calculated incrementally by specifying constant atomic N sources in the reference (unseeded) solutions, keeping both the radial transport properties and the upstream separatrix density constant. Full recycling of N impurities (as atoms) is used as an approximation for the plasma-wall interaction. To optimize these predictions, all simulations are performed with currents and cross-field drifts ($E \times B$, diamagnetic) activated.

3. MODEL-BASED RADIATION SCALINGS

Because of the high sensitivity of N radiation efficiency to the local electron temperature, T_e , a realistic solution for the initial divertor T_e distribution is important. In the absence of impurity seeding, the modelling with drifts yields low-recycling conditions for the outer divertor and high-recycling conditions for the inner divertor, with peak outer divertor temperatures $T_e \sim 40\text{eV}$ in ASDEX Upgrade and $T_e \sim 35\text{eV}$ in JET, compared to the significantly cooler inner target plasmas with $T_e < 20\text{eV}$ in both devices. This is in good agreement with the reported experimental conditions in JET, and a similar temperature asymmetry is measured in ASDEX Upgrade [1]. In both devices, the temperatures at which the radiation efficiency of N impurities is maximised ($T_e = 20\text{--}30\text{eV}$) are encountered primarily below the X-point, which localizes the radiation initially in the divertor, in between the X-point and the two targets.

Figure 1 shows the modelled radiated power fraction, $f_{\text{rad}} = P_{\text{rad}}/P_{\text{heat}}$, as a function of the N source rate. Here, P_{rad} is evaluated within the whole computational regime, and P_{heat} is the heating power applied at the core boundary ($\rho = 0.8$) in the simulations. In both devices, the radiation increases first in the inner divertor, starting from $f_{\text{rad}} < 10\%$ in the absence of seeding and evolving up to $f_{\text{rad}} \sim 30\%$. At this point, an abrupt transition is observed as the outer divertor begins to radiate, leading to $f_{\text{rad}} = 60\%$. No further increases are observed in the divertor radiated power, but f_{rad} continues to gradually increase due to increasing N core radiation. Another transition occurs when the core radiation suddenly leads to $f_{\text{rad}} > 90\%$. As a result, 3 different radiative regimes can be identified from the evolution of f_{rad} . In the following, we describe the qualitative differences between these regimes and discuss the physics behind the transitions.

3.1 REGIME 1 – INNER DIVERTOR RADIATION

In the first radiative regime, most of the radiation takes place in the inner divertor, which has the preferential temperatures for N radiation. The radiating species in the divertor are the lower N charge states, N^+ to N^{4+} , which are abundant in the regions of high electron density, n_e . The contribution of D neutrals is modest: $f_{\text{rad}} = 10\%$ in JET and $f_{\text{rad}} = 3\%$ in ASDEX Upgrade, and rather localized near the inner strike point. The total radiated power fraction increases with increasing N-seeding

rate, and the inner divertor radiation front moves from the near-target region towards the X-point. No significant changes are observed in the outer divertor, which has a high target temperature ($T_e > 35\text{eV}$) and a low radiated power.

Figure 2 shows the modelled n_e distributions in this first regime, indicating also the regions of strongest radiation. In both devices, a distinct region of high n_e is obtained near the inner target, radially outwards from the strike point. In ASDEX Upgrade, the electrons are accumulated near the strike point, whereas in JET they are distributed further away from the strike point, along and above the vertical target. Such density distributions are only modelled with activated $E \times B$ drifts, discussed further in [4]. The highest $E \times B$ drift velocities compared to the local parallel flow velocities are calculated (i) in the outer divertor, where the radial $E \times B$ drift brings particles across the separatrix, into the private flux region (PFR), (ii) in the PFR, where the poloidal $E \times B$ drift brings the particles from the outer strike point to the inner strike point, and (iii) in the inner divertor, where the radial $E \times B$ drift brings particles across the inner separatrix, radially outwards along the inner target. In JET, the radial drifts are strong along the entire inner target, whereas in ASDEX Upgrade the drifts are significant mostly close to the separatrix. This is likely a result of the inner divertor geometry, and a potential cause for the differences in the inner divertor n_e distributions.

3.2 REGIME 2 – MAXIMUM DIVERTOR RADIATION

Regime 2 is encountered when the outer strike point begins to cool down as a result of increasing N concentration. Two physical mechanisms come then into play and accelerate the cooling process: (i) the reduction of T_e increases the radiative efficiency of N impurities and (ii) parallel currents become weaker and reduce the heat fluxes entering the outer divertor [4]. A stable radiative regime is only obtained when the outer strike point has cooled down below 10eV. Regime 2 is characterized by high-recycling outer divertor conditions, increased neutral pressure in the divertor and radiation in both divertor legs. The radiation fronts are located in both divertor legs near the X-point, see Figure 3, where steep poloidal temperature gradients are produced. In this regime, the strongest $E \times B$ drifts are obtained near the X-point, and they no longer lead to a spreading of n_e along the inner target.

In regime 2, the divertor radiated power is maximised. The inner divertor contributes $f_{\text{rad}} \sim 30\%$ in JET and $f_{\text{rad}} \sim 30\text{--}35\%$ in ASDEX Upgrade, with radiation arising predominantly from the lower charge states, N^+ to N^{4+} . In the outer divertor, the same radiative species contribute $f_{\text{rad}} = 25\text{--}30\%$ in JET and $f_{\text{rad}} \sim 20\%$ in ASDEX Upgrade. The difference in outer divertor radiation is likely to arise from the differences in the available radiating volume between the two devices: The modelled upstream power decay length, λ_q , is smaller in ASDEX Upgrade (2mm) than in JET (7mm), and a similar difference is obtained for the outer divertor power spreading (Gaussian width $S = 0.4\text{mm}$ in ASDEX Upgrade, $S = 2.8\text{mm}$ in JET), calculated using the fitting formulas in [5]. In both devices, the higher charge states, N^{5+} and N^{6+} , contribute to core radiation, which increases approximately linearly with the N seeding rate, contributing to the slow evolution of f_{rad} .

3.3. REGIME 3 – MAXIMUM TOTAL RADIATION

As f_{rad} slowly increases, the outer divertor cools down further and the radiation front moves above the X-point. The radial $E \times B$ drift begins to bring N impurities inwards across the separatrix, and the radiative losses produced by N impurities increase on the closed field lines. Additionally, more heat is conducted radially outwards from the closed field lines, as the radial temperature gradients become steeper across the separatrix, leading to cooling of the plasma above the X-point. This yields the third radiative regime, characterized by an abrupt increase of f_{rad} above 70% and radiation just above the X-point, see Figure 4.

The transitions to both regime 2 and regime 3 are connected with a pressure loss along the open field lines (increasing by about 20% at each transition). When moving to the third regime, also the upstream pressure reduces (by about 20%), resulting in a significant (at least 50%) reduction in the target ion fluxes. Unlike in the transition to regime 2, the divertor neutral density is reduced in regime 3.

3.4. SCALING OF THE RADIATIVE SOLUTIONS

The above results are discussed in comparison to an experimental scaling law for P_{rad} [2]:

$$P_{\text{rad,div}} = 1720 p_{0,\text{div}}^{0.47} (Z_{\text{eff}} - 1)^{0.31} R^{1.095} \lambda_q^{1.148}, \quad (1)$$

where $p_{0,\text{div}}$ is the divertor neutral pressure and R is the major radius. Although this scaling is based on H-mode discharges, similarities can be expected with the present studies due to the similarity of the divertor regimes, particularly regarding the distribution of T_e . The f_{rad} corresponding to this scaling is calculated for both devices using the modelled $p_{0,\text{div}}$ in the PFR, below the X-point. The Z_{eff} is calculated as an average along a line-of-sight which crosses the simulation region above the midplane (corresponding to the H-5 line in ASDEX Upgrade; a similar line crossing the $\rho = 0.85$ flux surface is calculated for JET), yielding in the first two regimes $Z_{\text{eff}} = 1 - 2.5$ for AUG and $Z_{\text{eff}} = 1 - 1.4$ for JET, in line with the experiments. The upstream λq is calculated from the modelled unseeded discharges. Similar to [2], only the divertor radiation ($z < -0.68\text{m}$ in AUG and $z < -1.20\text{m}$ in JET) is taken into account.

Figure 5 shows the comparison with the modelled f_{rad} . We note first, that the scaled value of f_{rad} needs to be multiplied by a factor of 1.2 in order to get an agreement with the ASDEX Upgrade modelling results for regime 1. In JET, an opposite correction by a factor of 0.45 is needed, resulting in good agreement in both regimes 1 and 2 for the simulations with drifts included. The difference in scaling could be connected to the narrower upstream λq modelled for ASDEX Upgrade (2.2mm) compared to JET (7mm), which differs from the typical scaling assumption of a larger λq in ASDEX Upgrade [2]. The discrepancy when moving to regime 2 in ASDEX Upgrade could be due to an increase of radiation in both the inner and the outer divertor, leading to a larger increase of f_{rad} than predicted by the scaling law. In JET, nearly all of the radiation increase in regime 2 comes from the outer divertor.

The key parameter explaining the good agreement with the scaling law in JET is the divertor neutral density, which increases abruptly as the divertor transitions to a high-recycling regime, and then reduces in the third regime. The increase in Z_{eff} is more continuous throughout the three regimes. In regime 3, the DEMO-relevant high value of total f_{rad} , shown in Figure 1, is obtained because of an increased radiation in both the core and the SOL above $z = -1.2\text{m}$, which is not taken into account by the scaling law.

As shown in Figure 5, the experimental dependencies suggested by the scaling law can only be reproduced in simulations with drifts activated. This can be explained by the importance of drift terms in defining the properties of the radiative regimes and, thus, the parametric dependencies, as discussed in Sections 3.1–3.2. In the absence of drifts, the radiation in regime 2 is a factor of 2 lower in the inner divertor and a factor of 2 higher on closed field lines, leading to $\sim 50\%$ higher Z_{eff} than in simulations with drifts.

4. SUMMARY

The physics influencing the scaling of radiative divertor solutions in low-density JET and ASDEX Upgrade experiments was discussed, based on SOLPS5.0 simulations of N-seeding. The modelling indicates a sensitivity of the radiation distribution to the divertor asymmetries and divertor geometry. Cross-field drifts modify the radiation distribution obtained at a given radiated power fraction in both devices, as well as the parametric dependencies of divertor radiation. The divertor neutral density is a good scaling parameter in the present, strongly asymmetric divertor conditions at moderate radiated power fractions ($f_{\text{rad}} < 70\%$), but cannot describe further increases of f_{rad} .

ACKNOWLEDGEMENTS

This work was carried out within the framework of a Fusion Researcher Fellowship and the Power Plant Physics and Technology program of the European Fusion Development Agreement and Eurofusion Consortium (Task WP13-PEX-01-T01). The views and opinions expressed herein do not necessarily reflect those of the European Commission. The authors would like to thank D. Reiter and V. Kotov for their support and advice.

REFERENCES

- [1]. Aho-Mantila L. et al, 2013 Journal of Nuclear Materials **438**, Supplement(0) S321 – S325
- [2]. Kallenbach A., 2012 In 24th IAEA Fusion Energy Conference
- [3]. Schneider R. et al, 2006 Contributions to Plasma Physics **46**(1–2) 3–191
- [4]. Aho-Mantila L., 2014 In 41st EPS Conference on Plasma Physics
- [5]. Eich T. et al, 2011 Physical Review Letters **107**(215001)

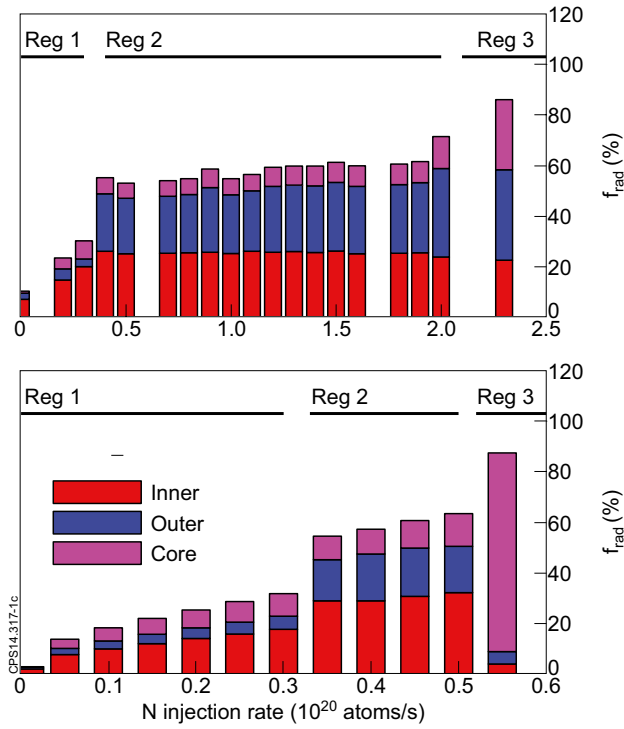


Figure 1: Simulated f_{rad} as a function of the N -seeding rate in JET (top) and ASDEX Upgrade (bottom). Inner = inner divertor, PFR and SOL, outer = outer divertor, PFR and SOL, core = closed field lines.

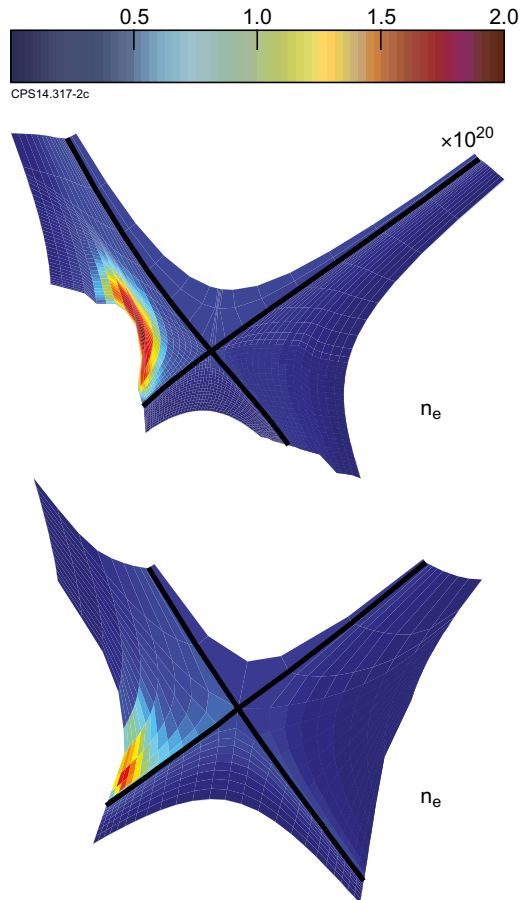


Figure 2: Simulated n_e distribution (m^{-3}) at $f_{rad} \sim 20\%$ in JET (top) and ASDEX Upgrade (bottom).

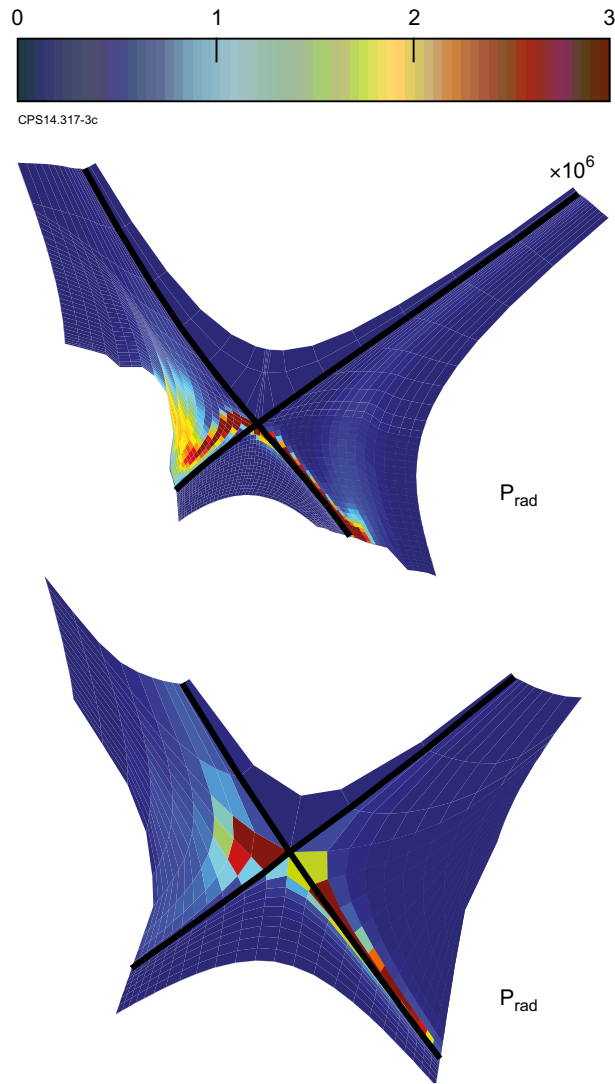


Figure 3: Simulated radiation power density (W/m^3) at $f_{\text{rad}} \sim 60\%$ in JET (top) and ASDEX Upgrade (bottom).

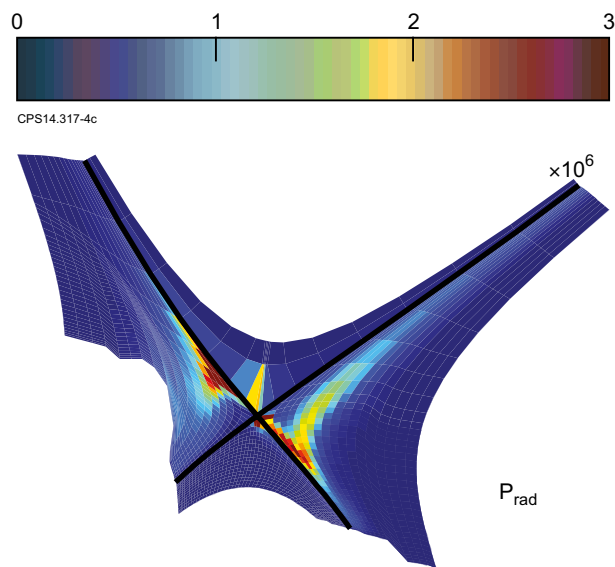


Figure 4: Simulated radiation power density (W/m^3) at $f_{\text{rad}} \sim 95\%$ in JET.

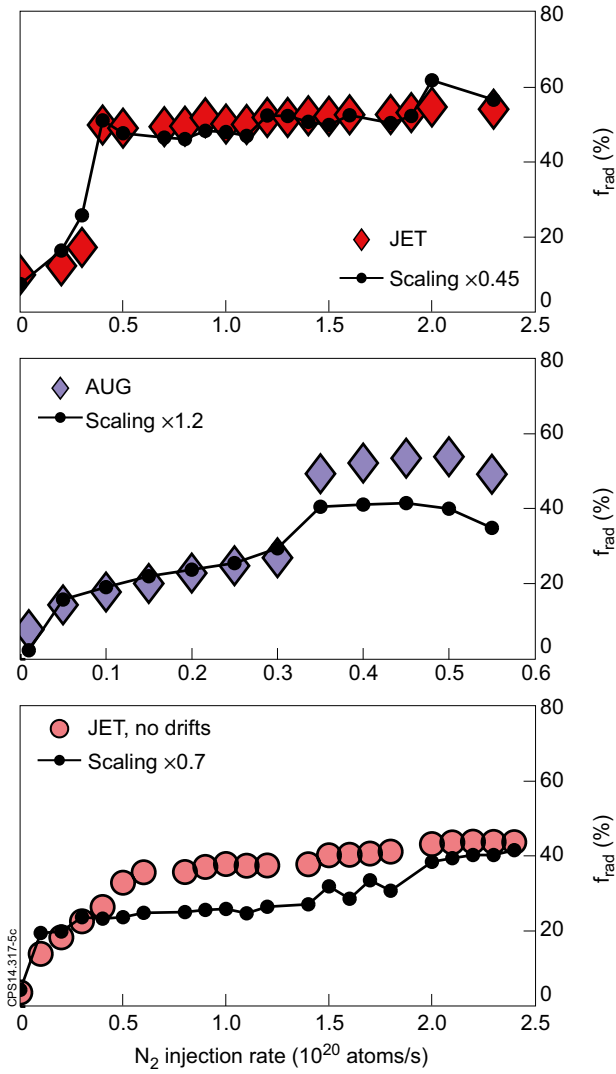


Figure 5: Simulated f_{rad} in the divertor, compared to f_{rad} calculated from the experimental scaling law, Equation (1).